Supporting Information

Effective Tailoring of MoS_2 layered number on the surface of CdS nanorods for Boosting Hydrogen Production Rate

Anjana E Sudheer[a], Pooja Varma[a], Assa Aravindh Sasikala Devi[b], D Amaranatha Reddy[a]*, D Murali[a]*,

[a]Department of Sciences, Indian Institute of Information Technology Design and Manufacturing, Kurnool- 518008, Andhra Pradesh India

[b]Nano and Molecular Systems Research Unit, University of Oulu, Pentti Kaiteran katu 1, 90570 Oulu, Finland

* Corresponding authors. E-mail: *dmurali@iiitk.ac.in, drreddy@iiitk.ac.in*

1.Experimental method

1.1 Synthesis of MoS_2 nanosheets (B- MoS_2)

High purity 2D MoS_2 nanosheets were prepared via a hydrothermal method. A typical preparation process involved dissolving stochiometric ratio of $Na_2MoO_4.2H_2O$ and C_2H_5NS using de-ionized (DI) water in a 100 mL volume Teflon lined autoclave. After magnetic stirring for three hours, the autoclave was placed inside a hot air oven and heated at 200 ^oC for 24 hours. After reaction time, the hot air oven is allowed to air cooled to reach the room temperature. Finally, the

black products were collected and washed several times with DI water and ethanol to remove the impurities such as Mo metallic clusters and then finally heated at 100 ^{o}C for 10 hours to obtain the final bulk sized MoS_2 nanosheets.

1.2 Synthesis of Thick layered MoS_2 nanosheets (T- MoS_2)

Thick layered MoS_2 nanosheets were fabricated through the process of ultrasonic assisted exfoliation technique using N-methyl 2-pyrrolidone (NMP) as a solvent. The above synthesized B-MoS_2 nanosheets (2 to10 wt.%) were dispersed in 20 mL of NMP solvent and sonicated for three hours. During the ultrasonication process, vibration energy will break the chemical bond between the layers in the B-MoS_2 nanosheets and form a thick layered MoS_2 nanosheets. To obtain final products, obtained black products were collected and washed several times with DI water and ethanol to remove the impurities and then finally heated at 100 ^{o}C for 10 hours.

1.3 Synthesis of H_2O_2 treated thin layered MoS_2 nanosheets (H-MoS_2)

Thin layered MoS_2 nanosheets were fabricated by etching of bulk MoS_2 nanosheets in presence of an oxidant using ultrasonic assisted layer exfoliation technique. For the chemical etching of bulk MoS_2 nanosheets, a solution prepared by uniformly mixing NMP and H_2O_2 with series of ratios (0:20, 1:19, 2:18, 3:17, 4:16, 5:15, 6:17, 7:13). The synthesized B-MoS_2 nanosheets were collected and transferred to the prepared solution and ultrasonicated for three hours. Chemical etching in presence of an oxidant (H_2O_2) create S-defects in thin layered MoS_2 nanosheets and it will help to increase photocatalytic activity of the material. After three hours of etching process, the final product obtained as thin layered MoS_2 nanosheets in the solution. The as prepared thin layered MoS_2 nanosheets were collected, washed several times with DI water and then dried at 100 ^{o}C for 10 hours.

1.4 Synthesis of CdS nanorods

CdS nanorods were fabricated using solvothermal method. For the synthesis of CdS nanorods, extra pure cadmium acetate (Cd $(CH_3COO)_2$ $2H_2O$) and thiourea (CH_4N_2S) were selected as precursors. For the dissolution of precursors, ethelenediamine selected as a solvent and it promoted the formation of nanorod structure. First step, the selected precursors were mixed in specific ratio and dissolved in 60 mL of ethelenediamine. The solution stirred using magnetic stirrer for uniform dispersion. After uniform dispersion, the solution was transferred to a 100 mL Teflon-lined autoclave placed inside a hot air oven. The time and temperature of reaction process were controlled to 48 hours and 160 ^oC respectively. After completing the reaction process, material was allowed for natural cooling. Then the material was collected and washed with DI water several times to remove the impurities. A yellow colored CdS material was formed and dried at 80 ^oC for 10 hours.

1.5 *Synthesis of CdS/B-MoS_2 nanostructures*

CdS/B-MoS_2 nanostructures were fabricated with aid of magnetic stirring. The above synthesized B-MoS_2 nanostructures were dispersed in 20 mL of de-ionized water and stirred for two hours. To the suspension of bulk sized MoS_2 nanosheets in DI water, desired amount of CdS nanorods were transferred and stirred for another three hours. After uniform mixing, the solution was filtered and the washed with DI water several times. Finally, CdS/B-MoS_2 nanostructures were collected and dried at 80 ^oC for 10 hours.

1.6 *Synthesis of CdS/T-MoS_2 nanostructures*

Ultrasonic assisted exfoliation technique was used for the synthesis of CdS/T-MoS_2 nanostructures. The above synthesized T-MoS_2 nanosheets dispersed in 20mL volume NMP

solution. For complete dispersion of T-MoS_2 nanostructure, solution was ultrasonicated for one hours. Then the suspension of T-MoS_2 nanosheets mixed with CdS nanorods and subjected to ultrasonication for two hours. After ultrasonication, the suspension was stirred for 12 hours at room temperature to make uniform interfacial contact between CdS and MoS_2 nanostructures. Then the solvent in the suspension was removed by vacuum distillation to collect CdS/T-MoS_2 nanostructures. The collected CdS/T-MoS_2 nanostructures washed in DI water to remove impurities and dried at 80 ^oC for 10 hours.

1.7 ***Synthesis of CdS/H-MoS_2 nanostructures***

To synthesize CdS/H-MoS_2 nanostructures, as-synthesized H-MoS_2 layered structure were collected and transferred to the solution of NMP and H_2O_2 mixed with series of ratios (0:20, 1:19, 2:18, 3:17, 4:16, 5:15, 6:17, 7:13) and ultrasonicated for one hour. To this black suspension of layered H-MoS_2 nanosheets, desired amount of CdS nanorods were quickly transferred and subjected to ultrasonication for another two hours. For the homogeneous dissolution of material in the solution, it was stirred for 12 hours at room temperature. After complete dissolution, solvent in the suspension was removed by vacuum distillation to form CdS/H-MoS_2 nanocomposite. Final product collected and washed several times with DI water to remove the impurities and then dried at 80 ^oC for 10 hours.

2. Computational Methodology

The DFT calculations were performed using Vienna Ab-initio Simulation Package (VASP) based on plane wave basis sets[1]. The interaction between electron and ion was described based on projected augmented wave method (PAW)[2]. Exchange and correlation effects in the pseudopotential reported using Generalised Gradient Approximation[3] (GGA) and Perdew-Burke-Ernzerhof (PBE) functional. Since PBE functional underestimate bandgaps, HSE06[4] functional were used to correctly reproduce experimental bandgaps. Brillouin zone sampling were performed with a k grid size of 16x16x1 and 16x16x16 for MoS_2 and CdS systems respectively for the geometrical optimization. A 650eV plane wave cut-off energy was chosen for the calculation. Along with strict energy and force convergence during full relaxation, convergence was checked with respect to vacuum layers as well. The lattice parameters and bandgap values are matching with reported theoretical and experimental values.

In order to model HER reaction, 4x4x1 supercells of MoS_2 and CdS nanowire were constructed with suitable k-points. For the calculation adsorption energy of single atom hydrogen, it was placed on top of S atom of MoS_2 surface and CdS surface.

3. CHARACTERIZATION

Microstructure properties of the synthesized photocatalyst was studied using JEOL JEM-2100F transmission electron microscope (TEM) with an accelerating voltage of 200 kV. Hitachi S-4800 field emission scanning electron microscope (FESEM) was used for the study of surface morphology of synthesized nanostructures. The atomic force microscopy (AFM) measurements were carried out using AFM Park NX7. The EPR Spectra was obtained from JEOL JES-TE100 ESR Spectrometer operating at Xband frequencies and having a 100 kHz field modulation. Crystal structure of the samples were verified by using Bruker D8 Advance X-ray diffractometer with a

Cu Kα X-ray source. Monochromated Al Kα X-ray source (hν = 1486.6 eV) with energy of 15 kV/150 W used to confirm the chemical composition of the heterostructure formed. For the optical absorption study Shimadzu UV-1800 double-beam 5 spectrophotometer was used. Hitachi F-7000 fluorescence spectrophotometer used for the Photoluminescence (PL) measurements which helped to understand the recombination rate in the newly synthesized photocatalysts.

3.1 Photocatalytic experiment to measure hydrogen evolution

Photocatalytic experiment was conducted in a 150 mL reactor with air tighted rubber septum to cover the top part of the reactor. Photocatalytic reaction medium was prepared with appropriate ratio of lactic acid and water (3:12) and desired amount of photocatalyst was dissolved in photocatalytic medium. Then, the photocatalytic reactor tightly closed and sealed with silicon rubber septum. To create an inert condition inside the reactor first air evacuated and then purged with argon for 30 min. Solar simulator was used as a light source for photocatalytic reactions. The light intensity of solar simulator calibrated to 100W/m^2 (1Sun) using 15151 low cost calibrate Si reference cell. The evacuated reactor irradiated for 3 hours and evolved gases were analyzed using an off-line gas chromatograph equipped with 5 Å molecular sieve column and thermal conductivity detector. Caliberation of Gas chromatograph (G.C) was done with 10 % standard hydrogen. An amount of 100 µL evolved hydrogen gas collected using gas tight syringe through rubber septum and injected into the GC to estimate the quantity of evolved hydrogen. The quantum efficiency also calculated from the measured hydrogen using the equation below.

$$QE = \frac{Amount\ of\ hydrogen\ evolved\ \times 2}{Number\ of\ incident\ photons} \times 100$$

3.2 Photoelectrochemical experiments:

Photo electrochemical experiments were conducted in a three-electrode system (working electrode, counter electrode and reference electrode) using a Biologic 150-e electrochemical workstation. A solar simulator provided with A.M.1.5G filter and 150 W xenon lamp was used as light source to generate monochromatic illuminating radiation. The output light intensity was adjusted to 1 sun (100 W/m^2) using 15151 low-cost calibrated Si reference cell. The Ag/AgCl electrode and Pt wire were used as reference electrode and counter electrode respectively and 0.5M Na_2SO_4 aqueous solution selected as electrolyte in this PEC experiment. The pH value of electrolyte measured to be 6.72. To prepare the working electrode, as-prepared 10 mg of CdS, CdS/T-MoS_2 and CdS/H-MoS_2 heterostructures were dispersed into ethanol and nafion mixture. The mixture stirred using ultrasonic stirrer for two hours to obtain uniform suspension. After that, the suspension was slowly dropped into the Fluorine doped tin oxide (FTO) glass substrate and then dried at 80 ^oC for 3 hours in hot air oven. Photo responses were measured at 0.0 V during on-off cycling of the solar simulator. The electrochemical impedance spectroscopy (EIS) was carried out at open circuit potential over the frequency range of 10^5 to 10^{-1} Hz with a 5mV AC voltage. In addition to that, to calculate the flat band potential of CdS and MoS_2 nanostructures, Mott-Schottky plots at a frequency of 1 KHz examined using a standard potentiostat equipped with impedance spectra analyzer in the same electrolyte solution and electrochemical set up under dark condition. The obtained potential verses Ag/AgCl were switched to Normal Hydrogen Electrode (NHE) scale using the general equation $E_{NHE} = E_{Ag/AgCl} + 0.197$ V.

4. Supporting Figures

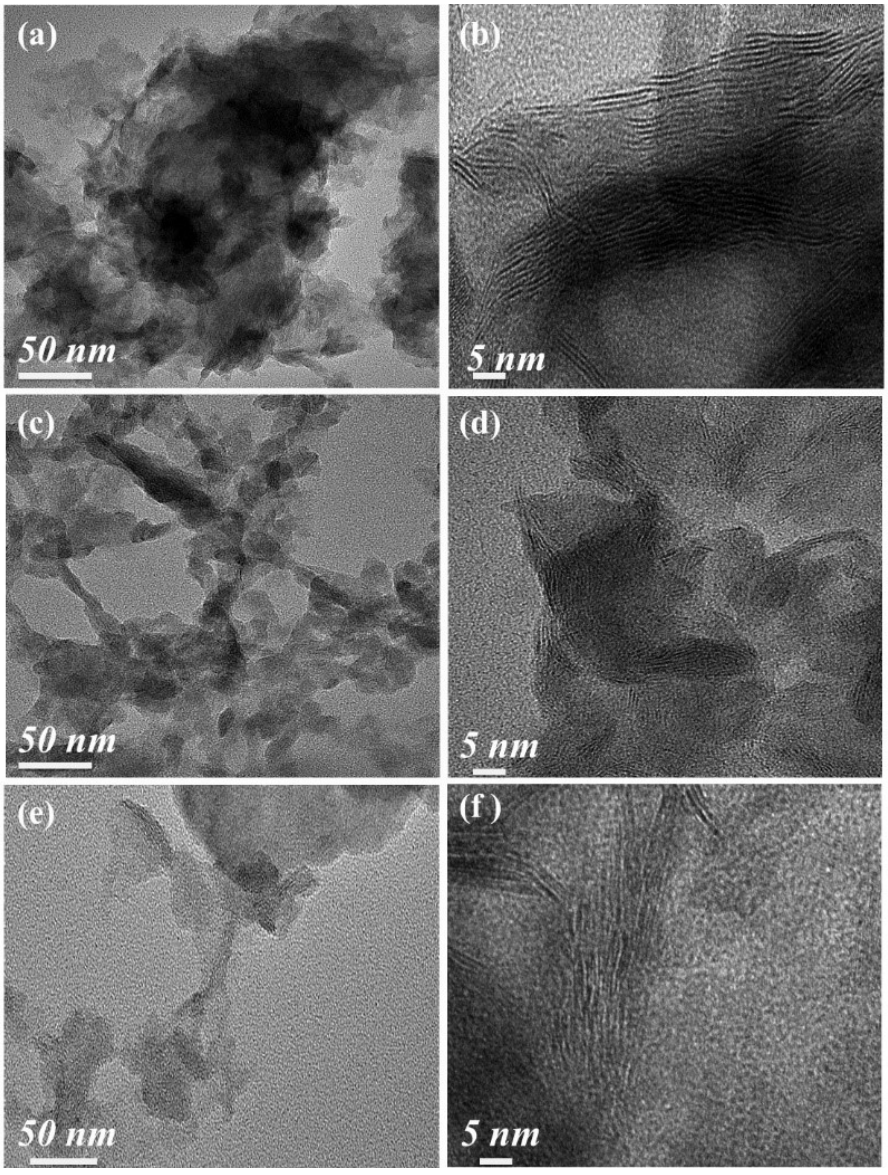

Fig. S1: FE-TEM and High-resolution TEM micrographs of synthesized MoS_2 nanosheets. B-MoS_2 nanosheets (a, b). T-MoS_2 nanosheets (c, d). H-MoS_2 nanosheets (e, f).

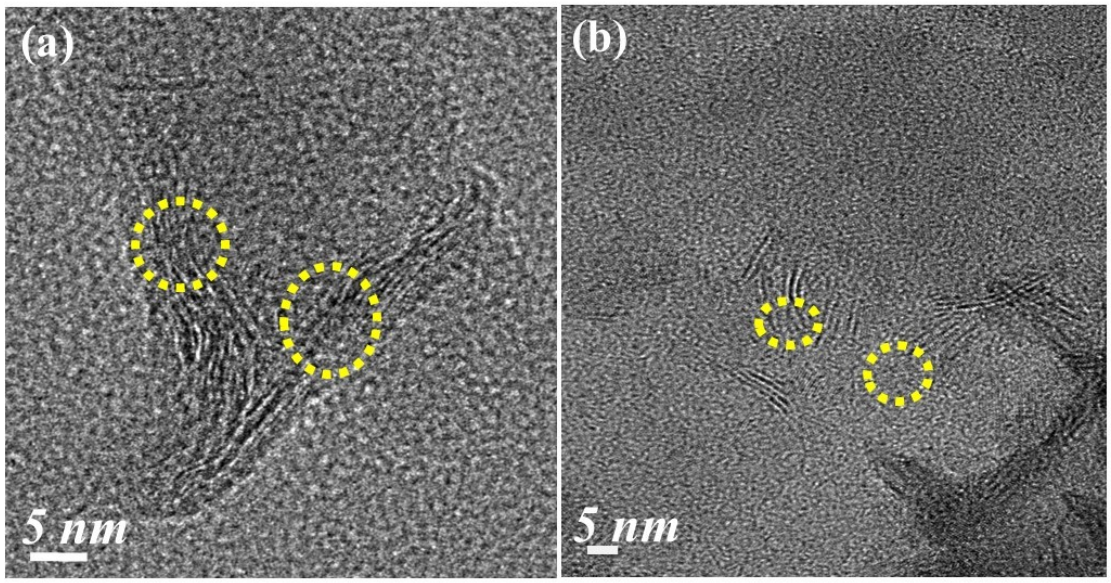

Fig. S2: FE-TEM images of breakage of H-MoS_2 nanolayers during the ultrasonic exfoliation process using H_2O_2 and NMP in 3:17 ratio.

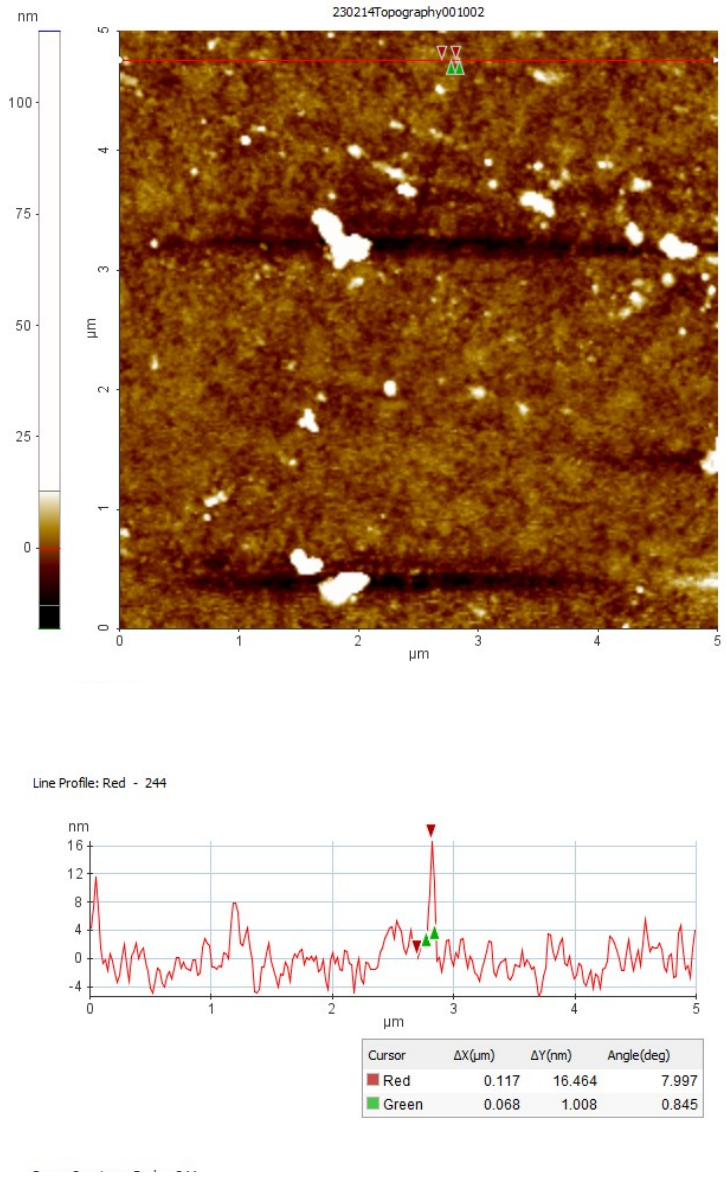

Fig. S3: AFM analysis of surface morphology of H-MoS_2 nanosheet (a). Line profile indicating thickness of H-MoS_2 nanosheets (b).

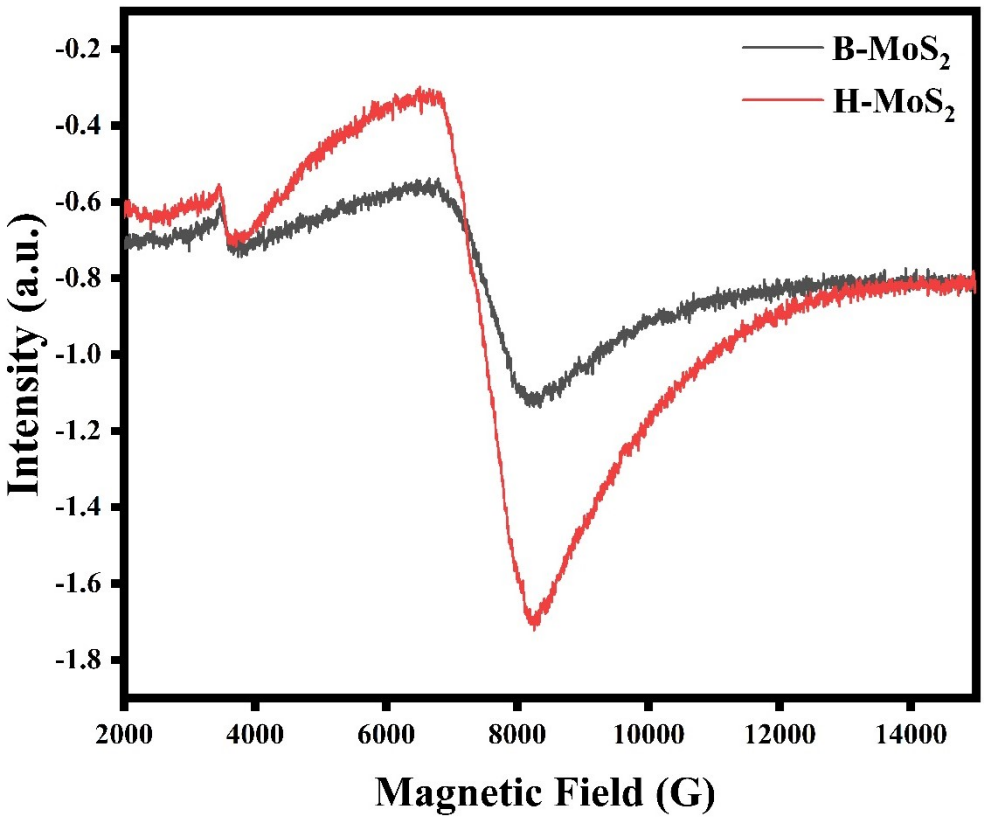

Fig. S4: EPR Signal of the sulfur vacancy of B-MoS_2 and H-MoS_2

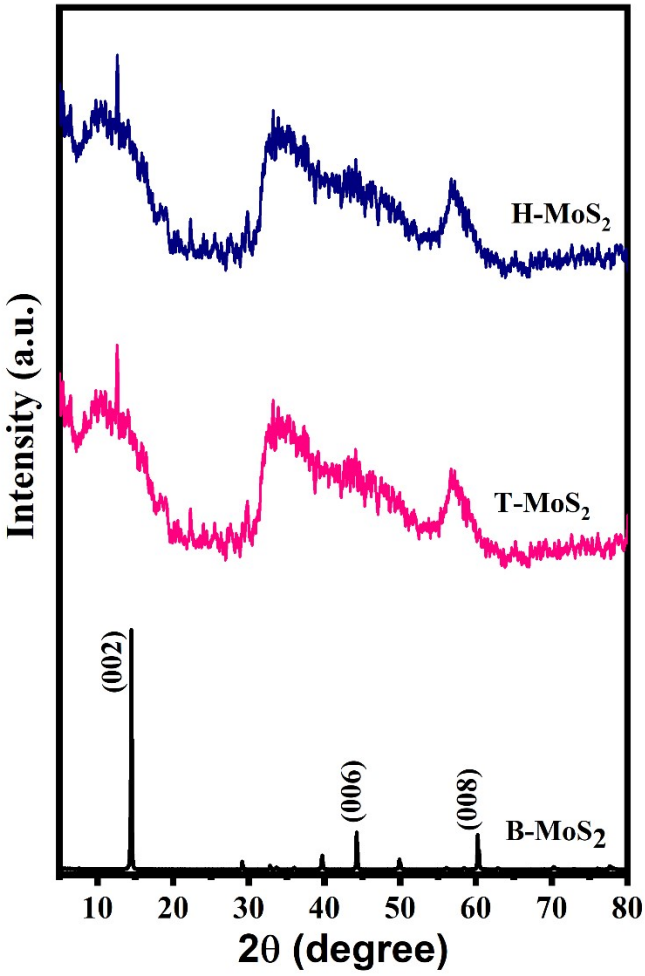

Fig. S5: XRD pattern of B-MoS_2, T-MoS_2 and H-MoS_2 nanosheets.

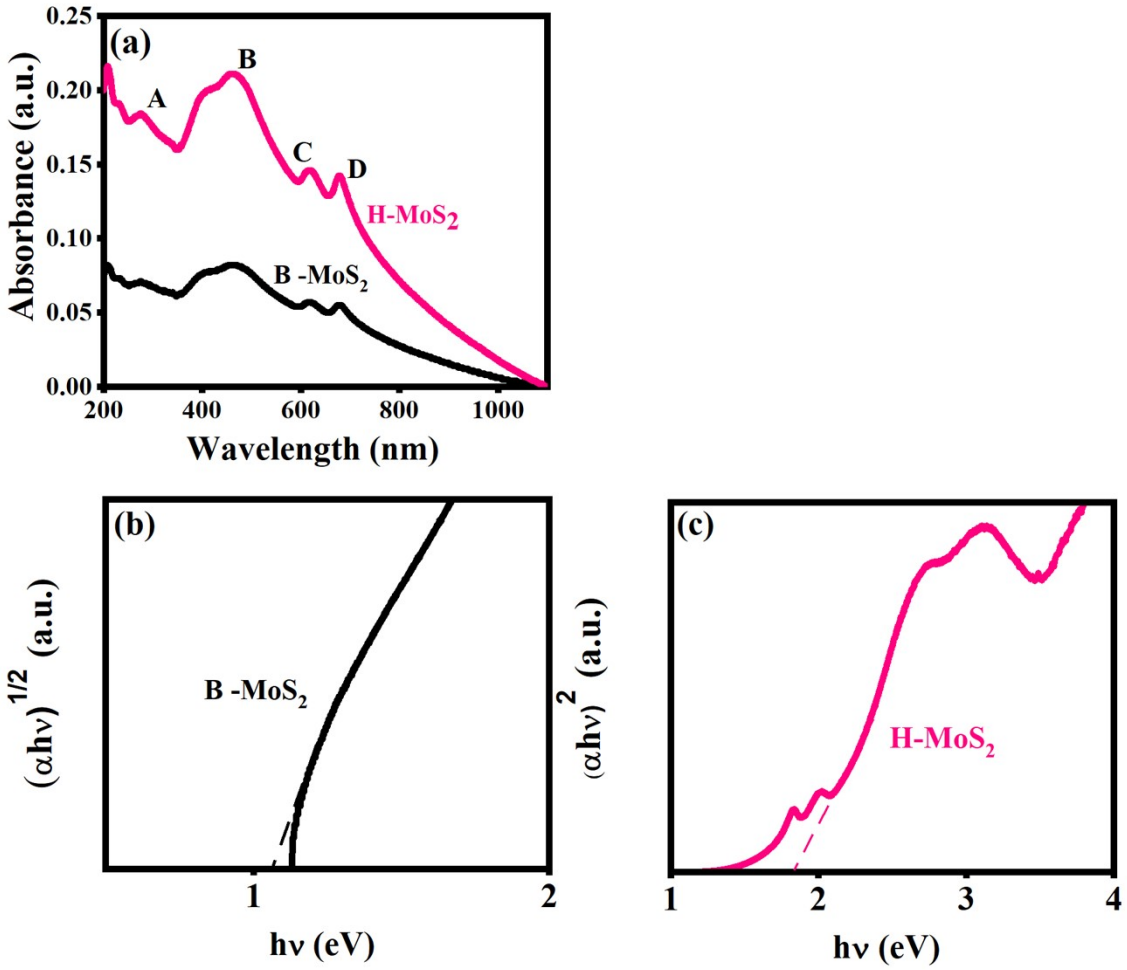

Fig. S6: UV-Vis absorbance spectra of B-MoS_2 and H-MoS_2 nanosheets (a). Tauc plot of B-MoS_2 and H-MoS_2 (b, c).

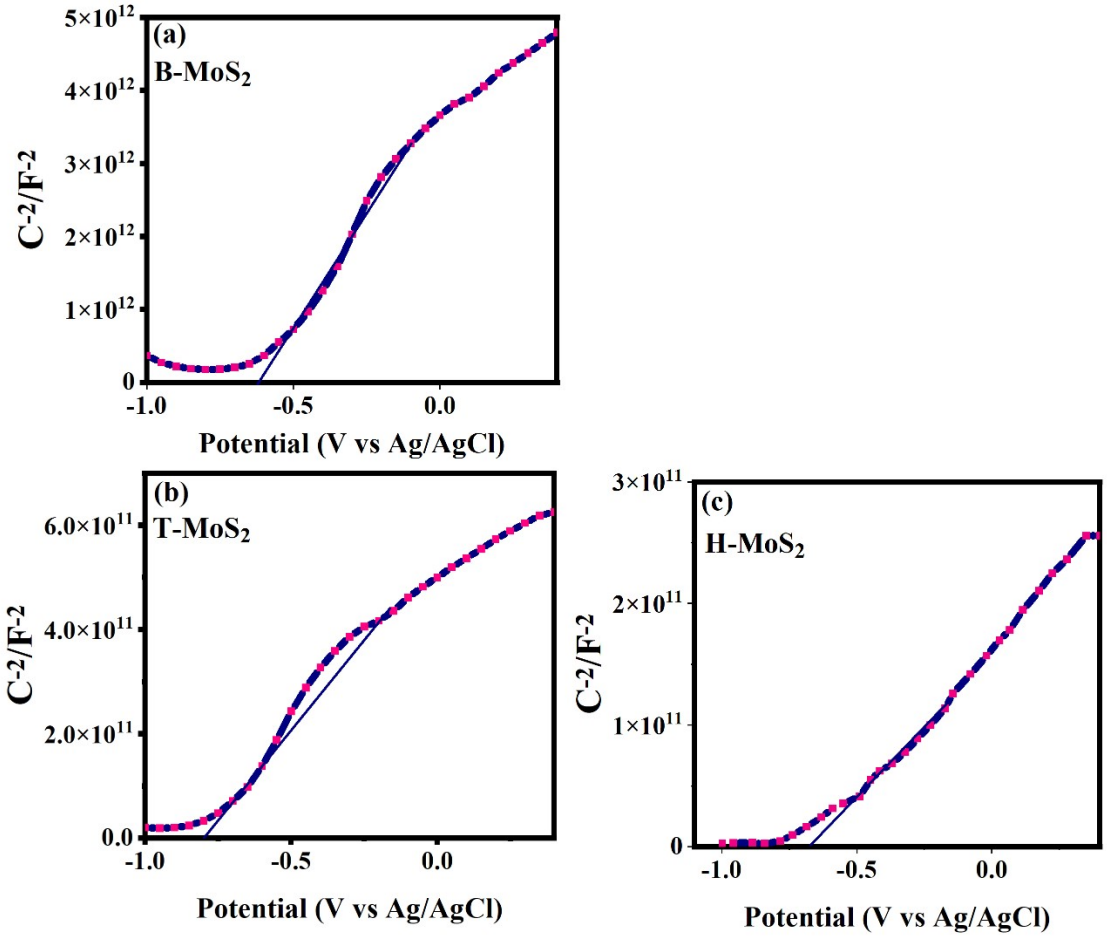

Fig. S7: Mott-Schottky plot of B-MoS_2 (a) T-MoS_2 (b) and H-MoS_2 (c) nanosheets.

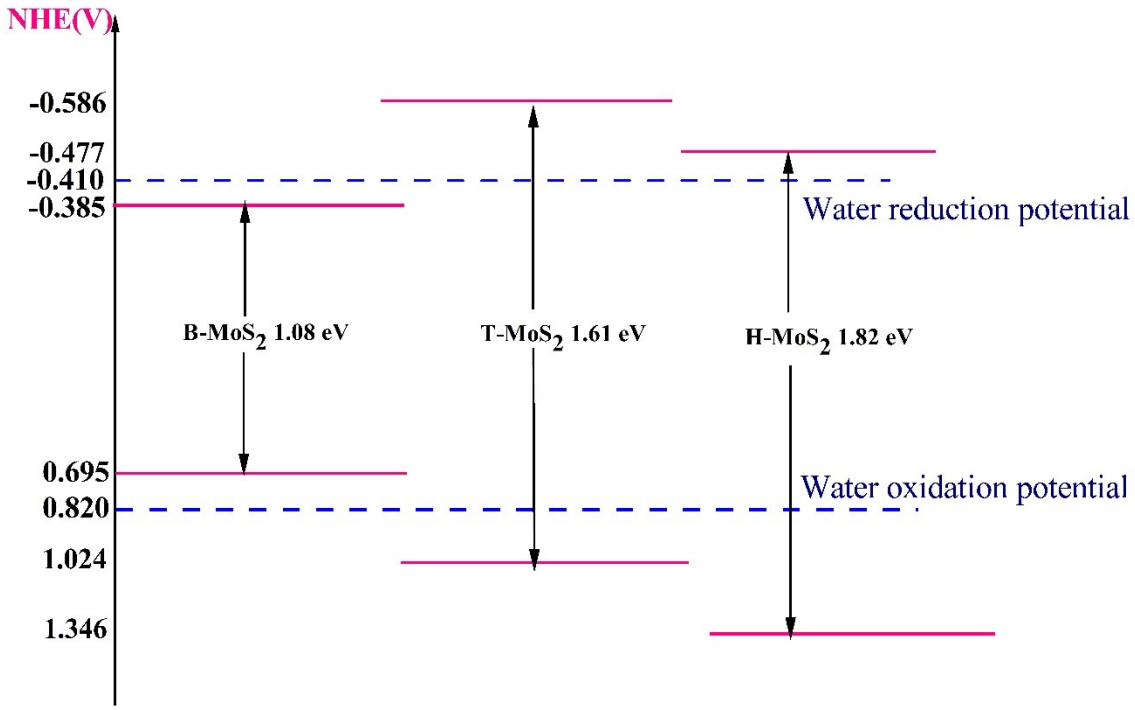

Fig. S8: Schematics for the comparison of band alignment of B-MoS_2, T-MoS_2 and H-MoS_2 nanosheets.

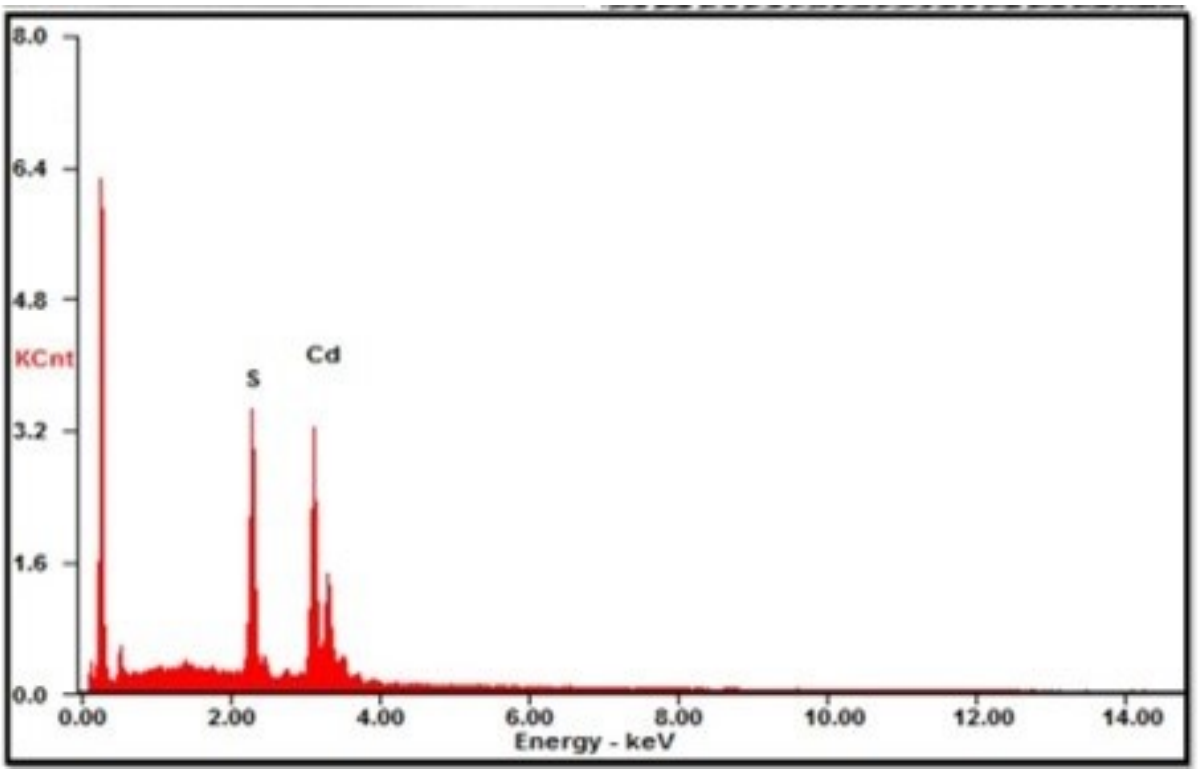

Fig. S9: Energy dispersive X-ray spectroscopy (EDS) line spectra of CdS.

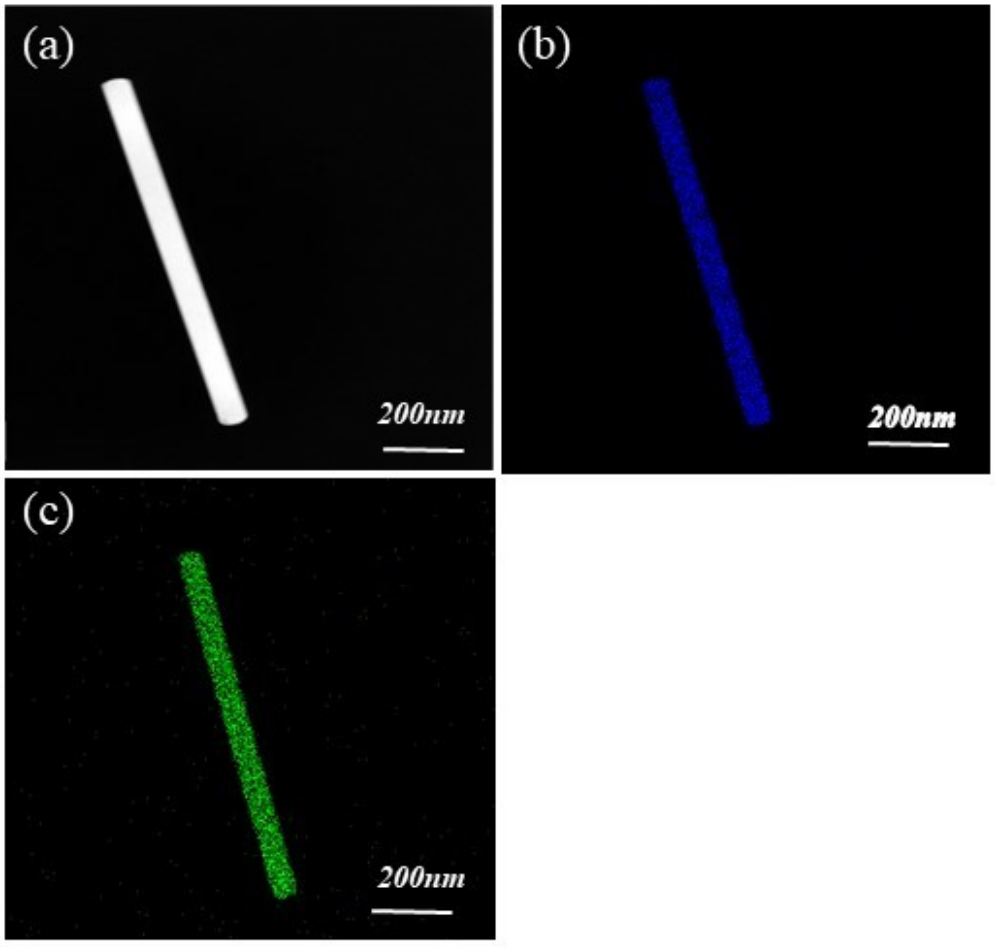

Fig. S10: Energy dispersive X-ray spectroscopy (EDS) mapping images of CdS nanorods. Electron micrograph (a), micrographs of Cd and (b) S (c) elements.

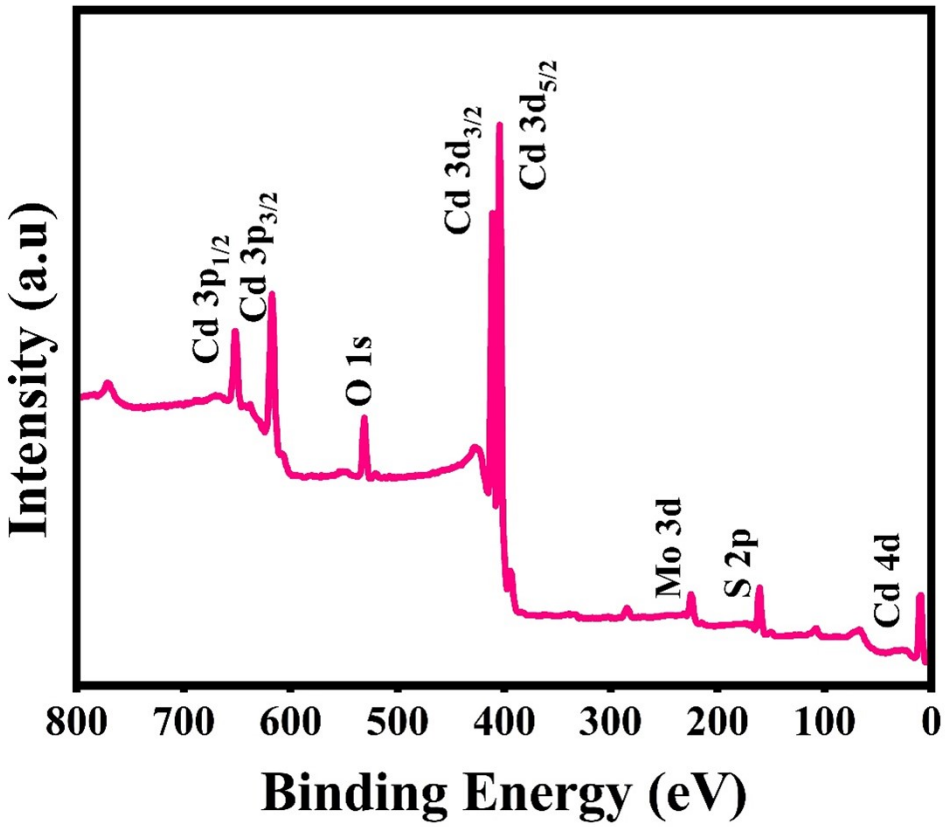

Fig. S11: XPS survey spectrum of CdS/H-MoS_2 photocatalyst.

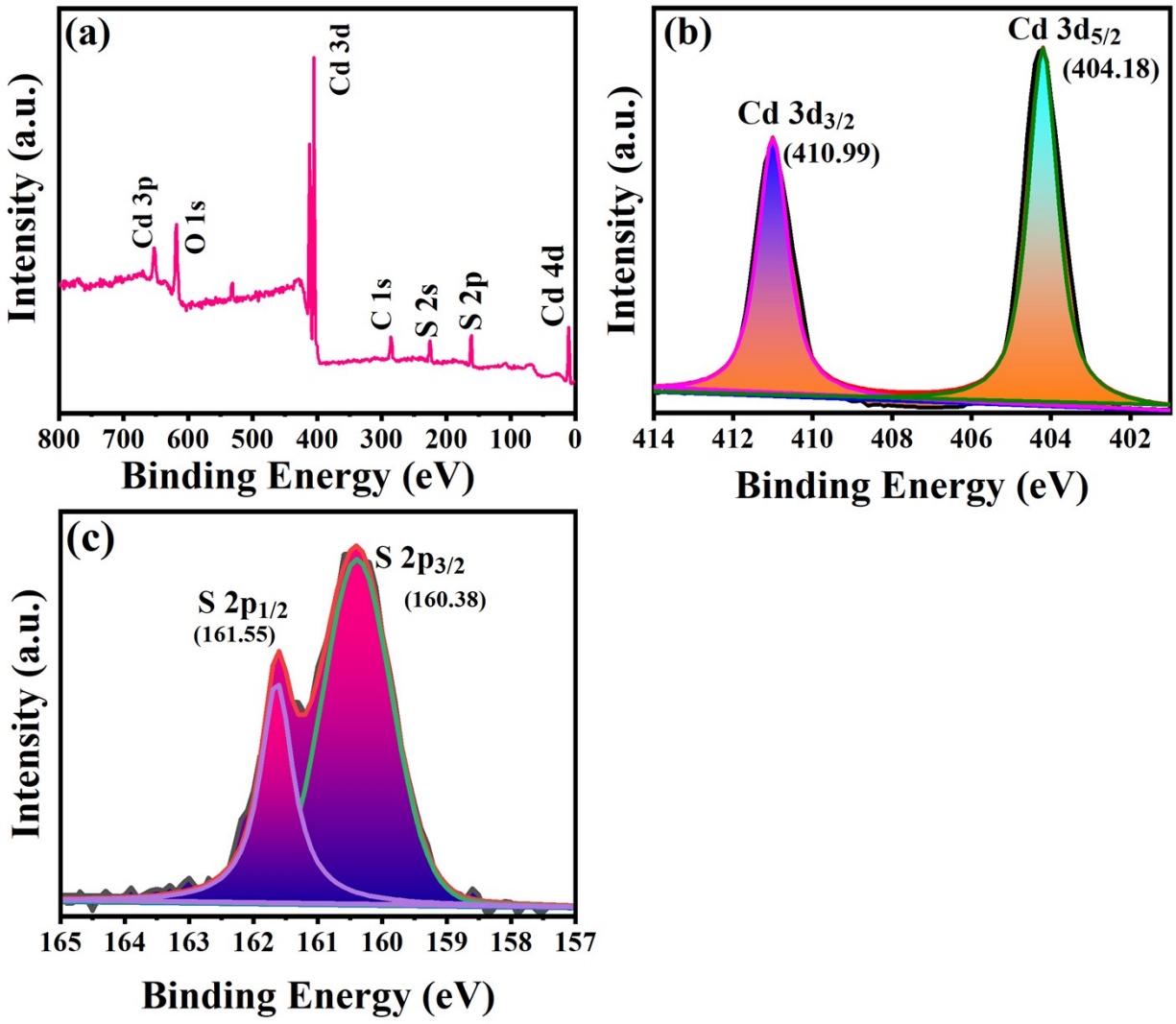

Fig. S12: XPS Survey spectra of CdS (a), XPS spectra of Cd 3d (b) and S 2p (c).

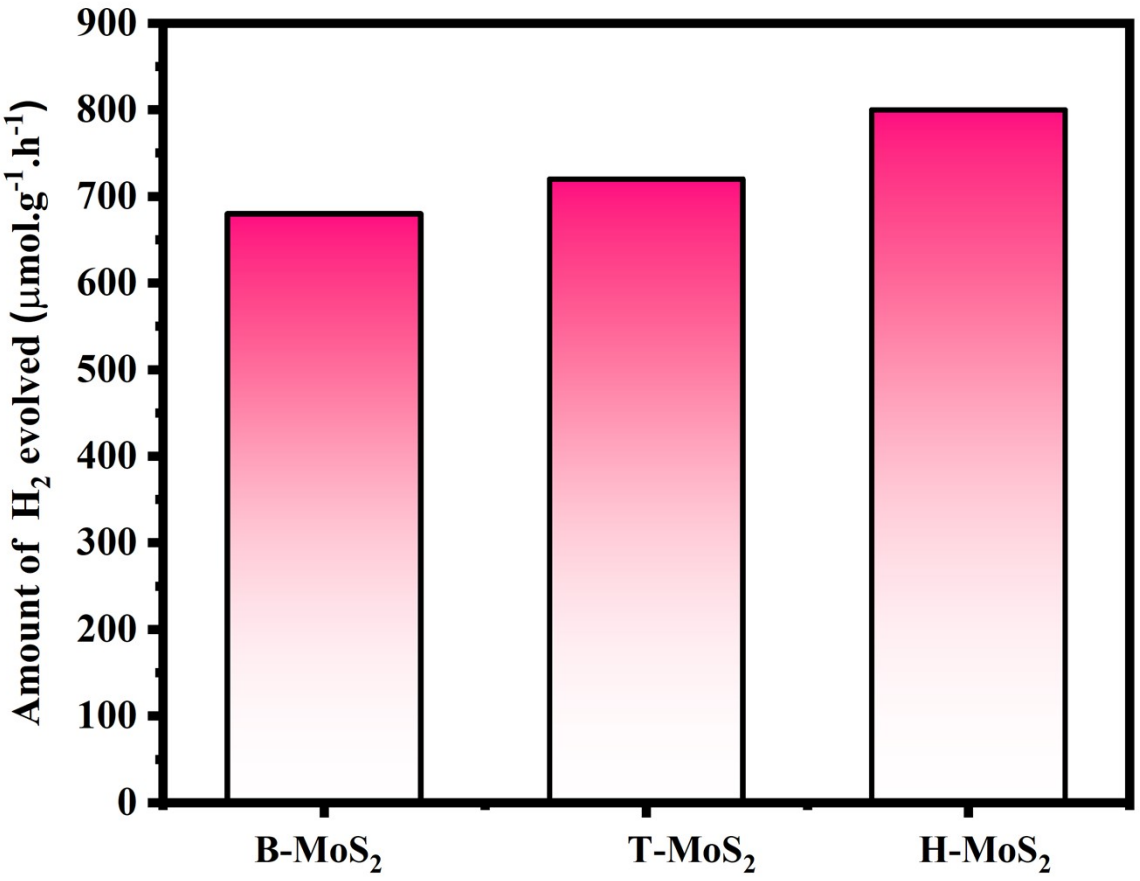

Fig. S13: Comparison data of the amount of hydrogen evolved from B-MoS_2, T-MoS_2 and optimized H-MoS_2 nanostructures.

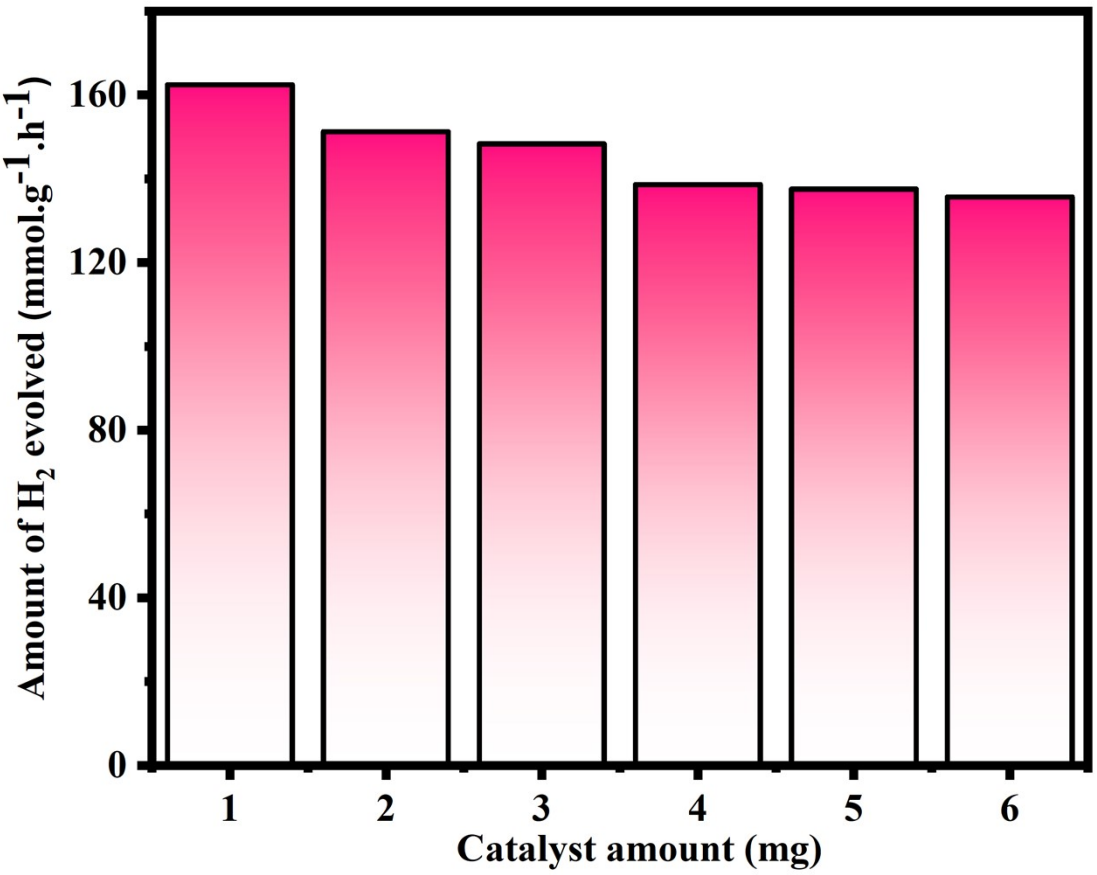

Fig. S14: Amount of hydrogen evolved by varying the amount of photocatalyst in photocatalytic reaction medium.

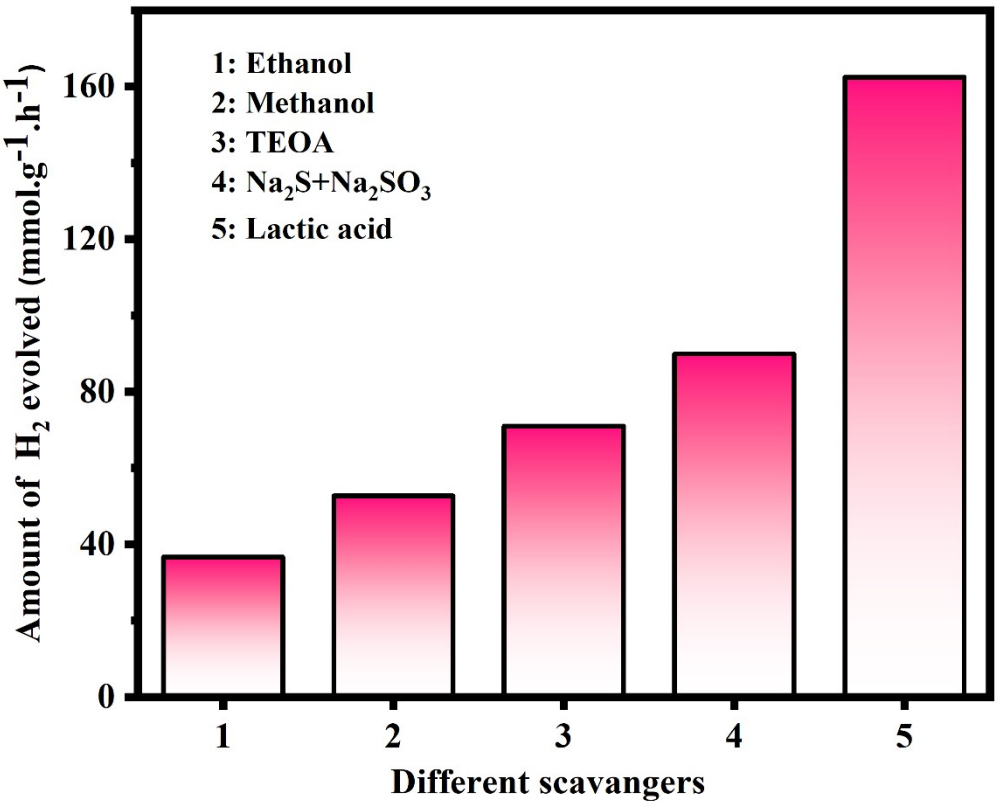

Fig. S15: Amount of hydrogen evolved in photocatalysis reaction process by experimenting with different sacrificial agents

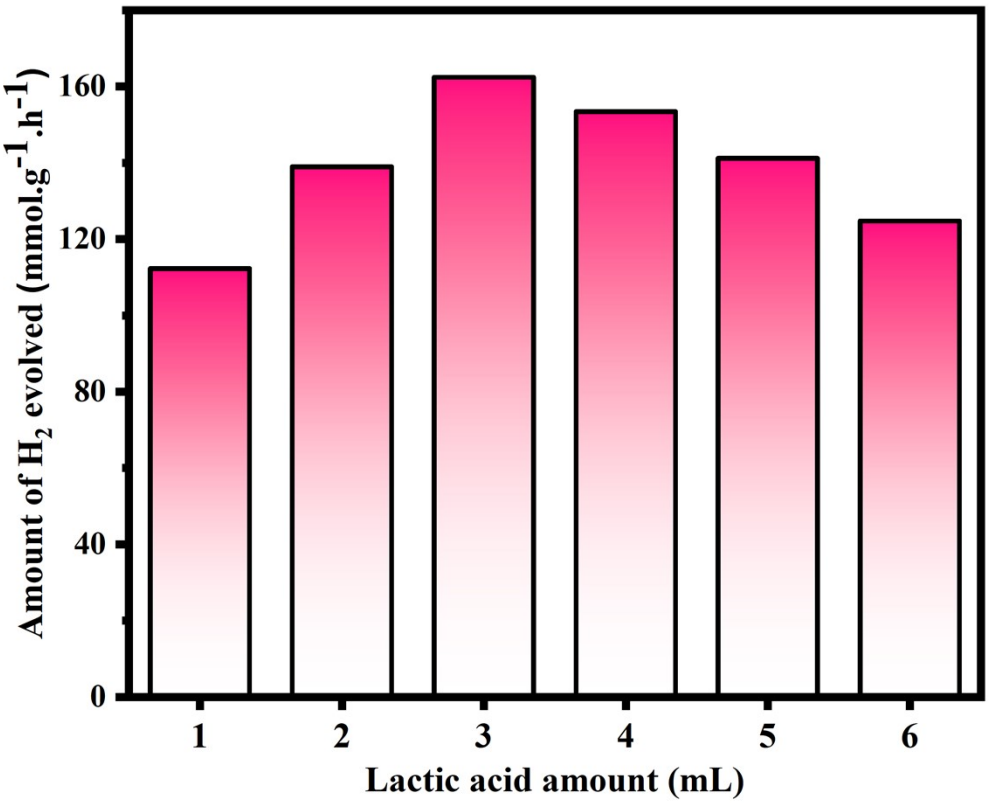

Fig. S16: Amount of hydrogen evolved from CdS/H-MoS_2 by varying the amount of lactic acid in photocatalytic reaction medium.

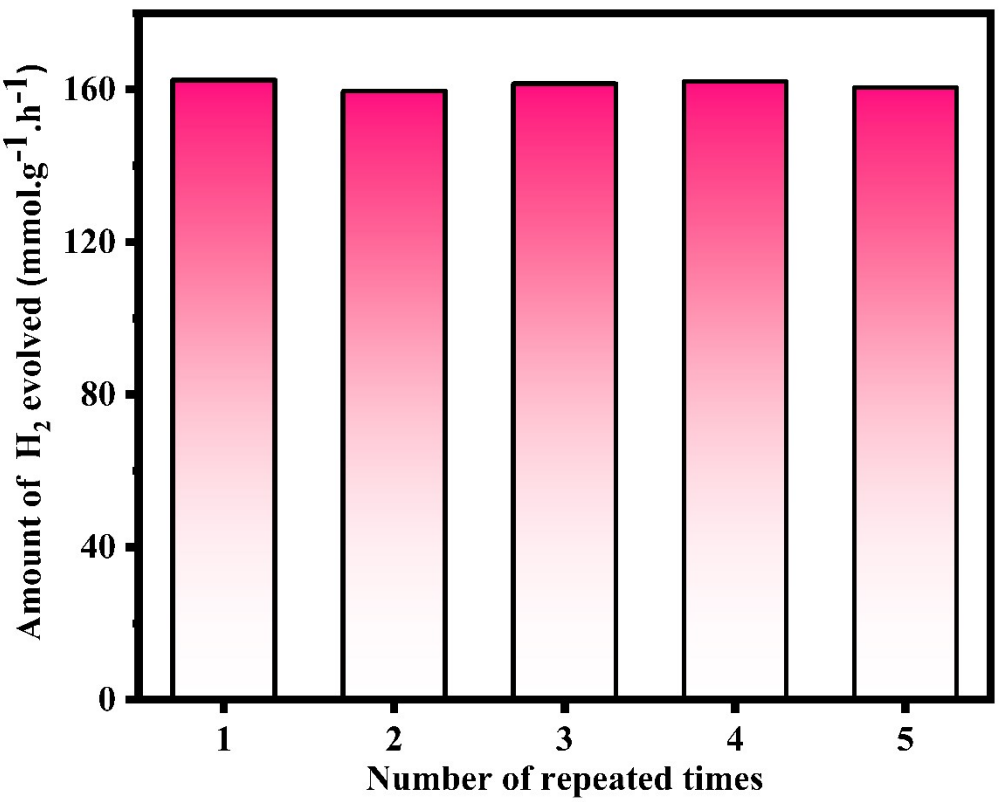

Fig. S17: Amount of hydrogen evolved from CdS/H-MoS_2 by repeating the experiment in same experimental conditions.

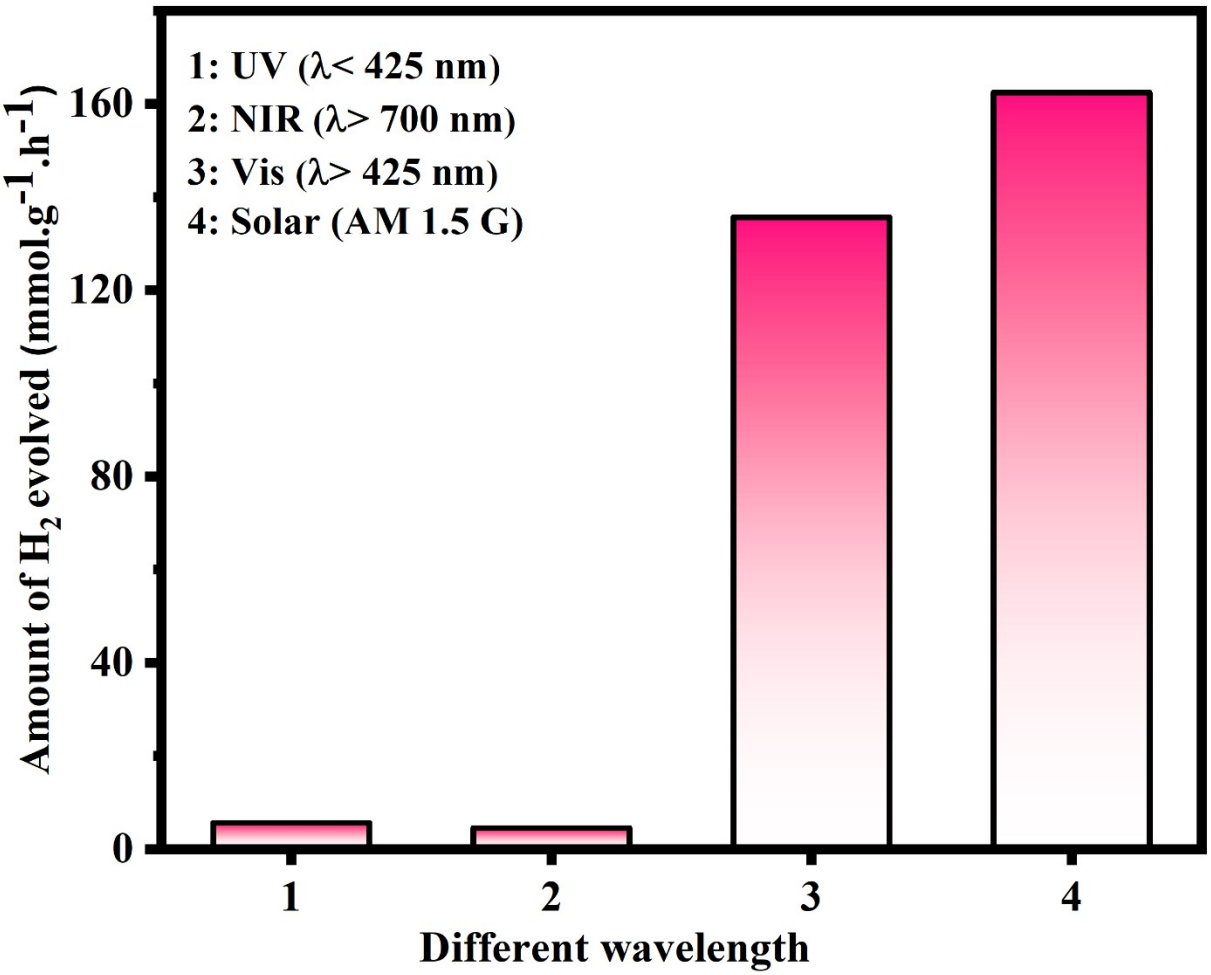

Fig. S18: Amount of hydrogen evolved from CdS/H-MoS_2 in the photocatalytic experiment conducted in different range of solar spectra.

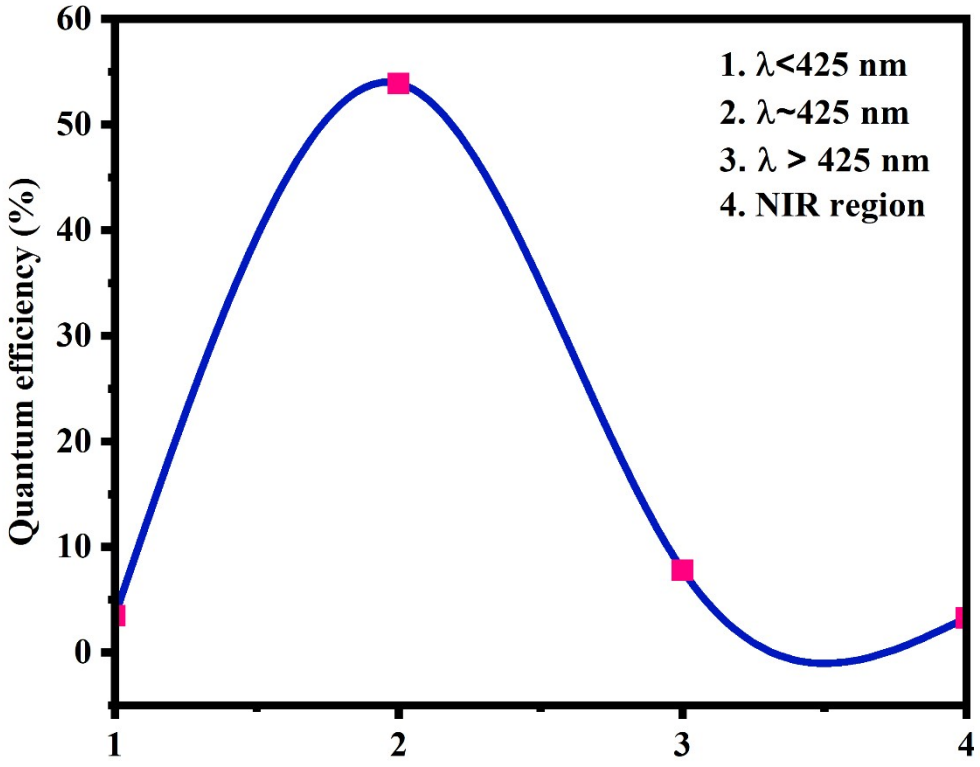

Fig. S19: Quantum efficiency of photocatalyst performed in the different regions of solar spectra.

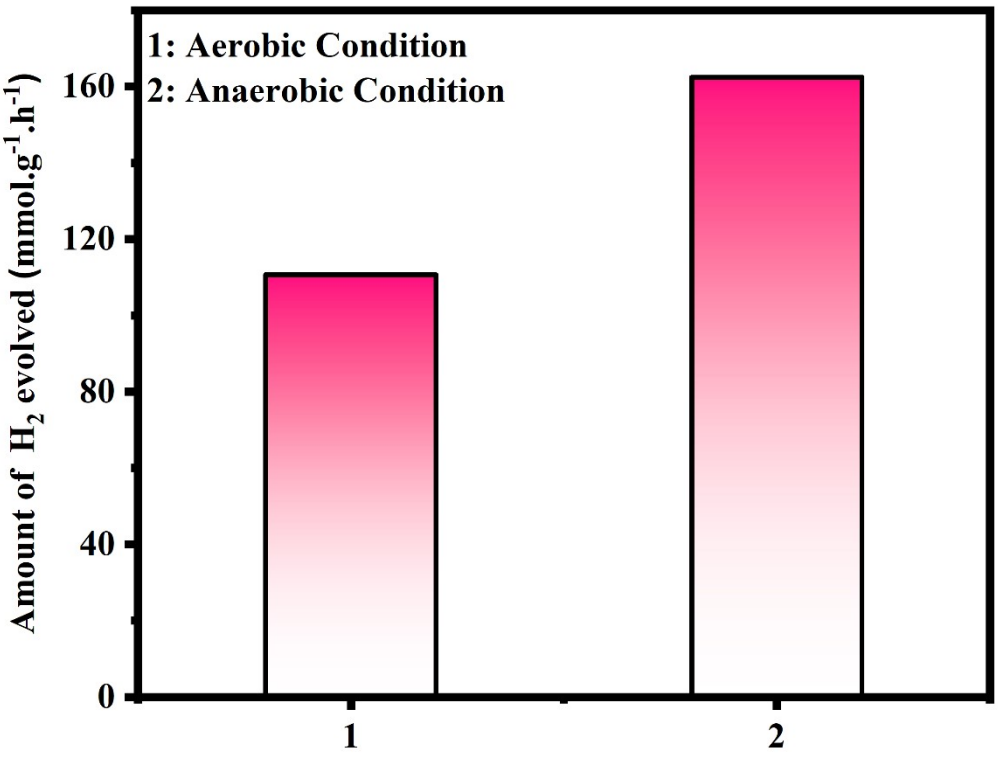

Fig. S20: Amount of hydrogen evolved in photocatalytic experiment in aerobic and inert condition.

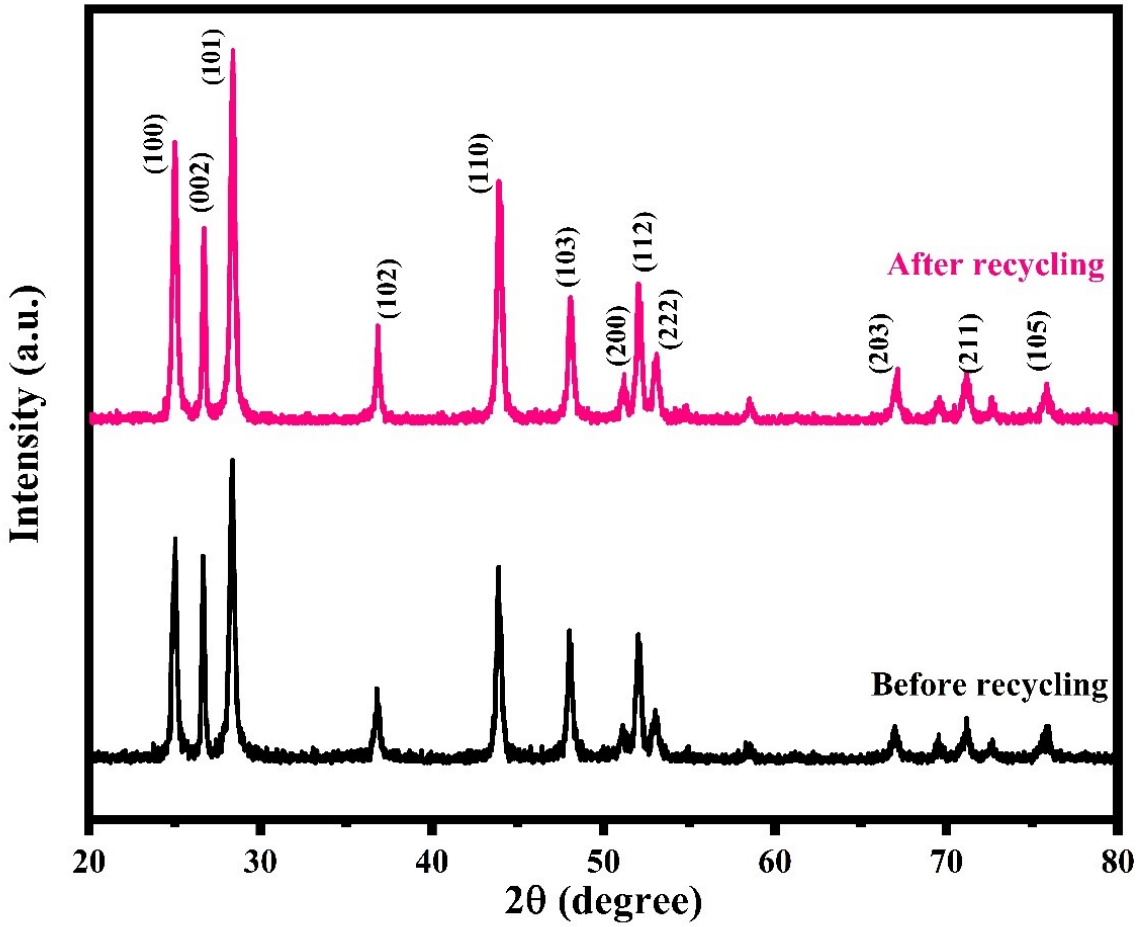

Fig. S21: XRD patterns of CdS/H-MoS_2 before and after recycling.

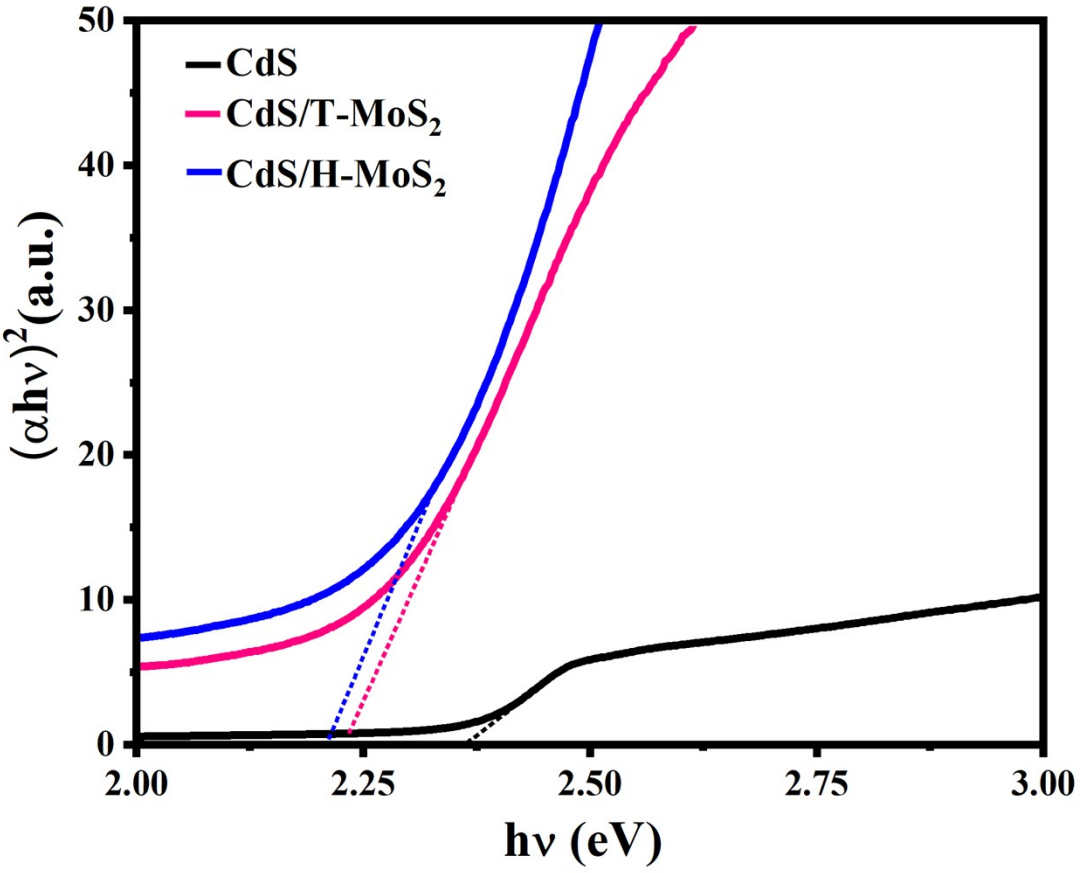

Fig. S22: Tauc plot for the bandgap comparison of CdS, CdS/T-MoS_2 and CdS/H-MoS_2.

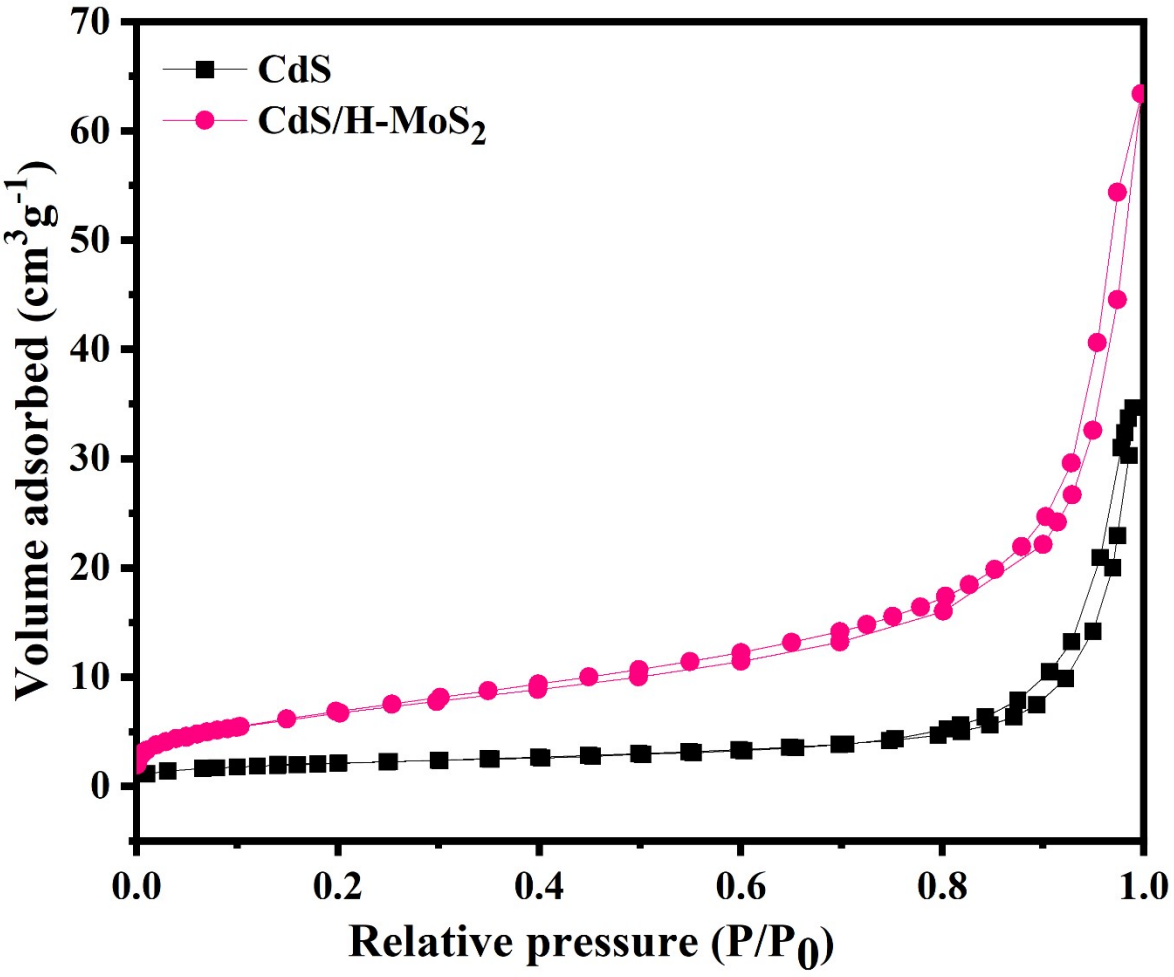

Fig. S23: Typical N_2 gas adsorption-desorption isotherms of CdS, CdS/H-MoS_2 photocatalysts.

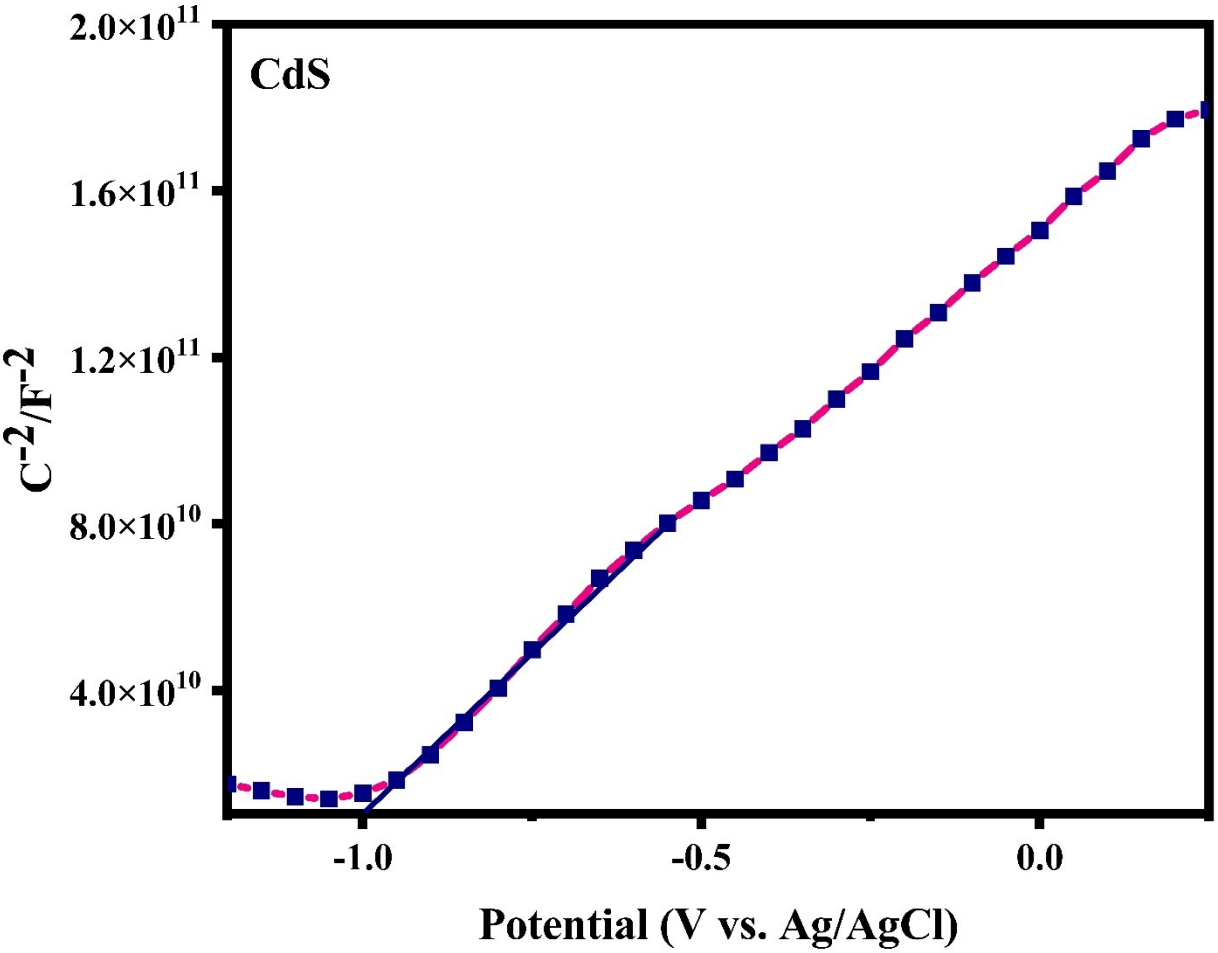

Fig. S24: Mott-Schottky analysis of CdS nanorods.

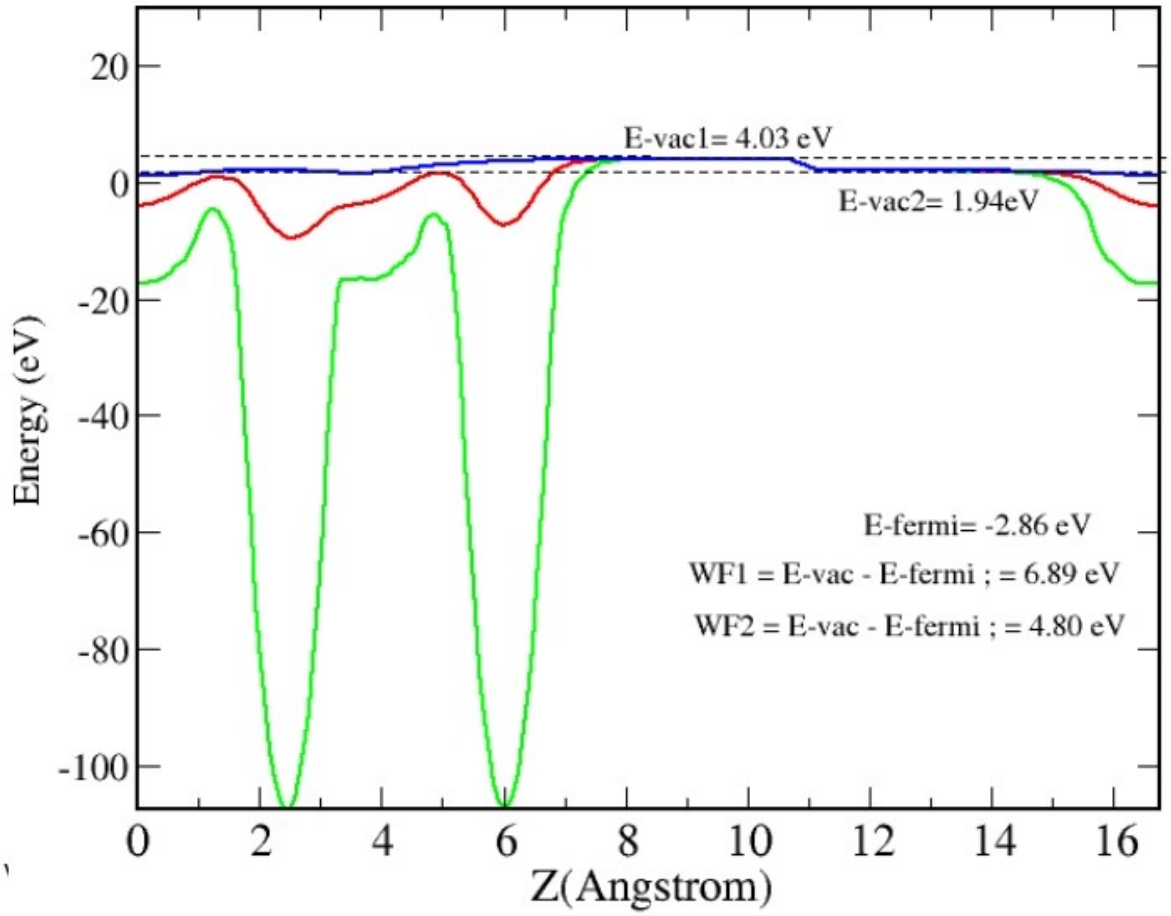

Fig. S25: Electrostatic potential diagram of CdS.

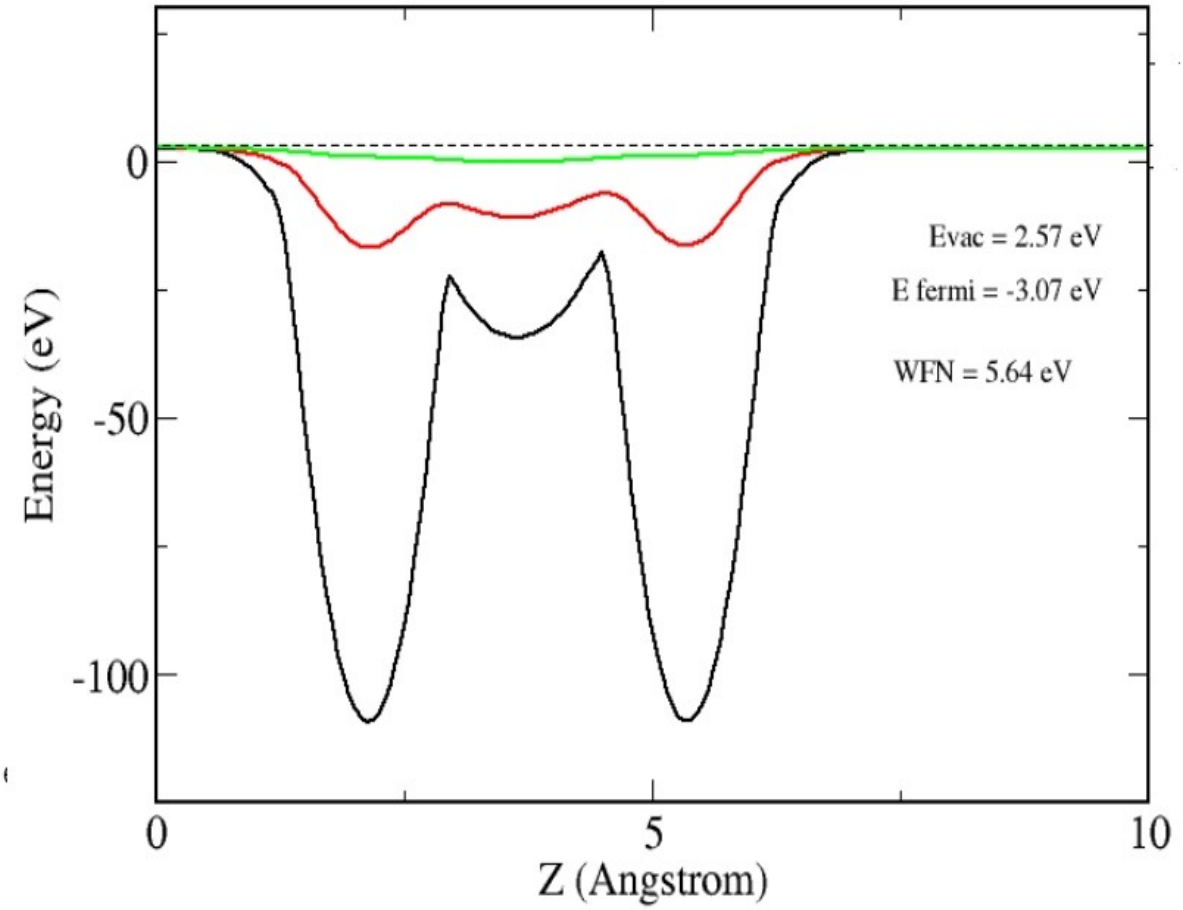

Fig. S26: Electrostatic potential diagram of MoS_2.

Table S1: HER comparison data of different CdS based photocatalysts

S. No	Photocatalyst	Light Source	Scavenger	Amount of Hydrogen evolution (mmol g^{-1} h^{-1})	Reference
1	CdS/H-MoS_2	Solar light	Lactic acid	160	Present work
2	CdS/CuS	Solar light	Lactic acid	0.561	[5]
3	CdS/C@CoS_2	Solar light	Lactic acid +TFA	87.73	[6]
4	CdS_2/WS_2/MoS_2	400 W Xe lamp	Lactic acid	19.2	[7]
5	$BiFeO_3$/CdS	Visible	No sacrificial agent	.421	[8]
6	$BaTiO_3$/CdS	Visible	Na_2S/Na_2SO_3	.483	[9]
7	CdS/ZnS-Pt	300 W Xe lamp.	Na_2S/Na_2SO_3	4	[10]
8	CdS/MoS_2	300 W Xe lamp.	Na_2SO_4	.4931	[11]
9	CdS/MoS_2/MWCNT	300 W Xe lamp.	Lactic acid	.676	[12]
10	CdS/Cu_7S_4/MoS_2	300W Xe lamp	Na_2S/Na_2SO_3	3.5	[13]
11	Core/Shell CdS/g-C_3N_4	Visible	Na_2S and Na_2SO_3	4	[14]

12	CdS/Cd	visible	Na_2S and Na_2SO_3	.1179	[15]
13	CdS/ NiS	visible	Lactic acid	18.1	[16]
14	CdS/NiS	300W Xe lamp	Na_2S and Na_2SO_3	49.2	[17]
15	CdS/CdSe	visible	Ascorbic acid	.015	[18]

Table S2: The optimized lattice parameters of CdS and MoS_2.

Structure	**Lattice parameters**	
	a (Å)	**c (**Å)
CdS	4.182	6.746
MoS_2	3.190	14.879

Table S3: Total energy of CdS, CdS-H, MoS_2, MoS_2-H, Single H atom using Density Functional Theory calculations.

	Total energy
CdS	-272.71683803
CdS-H	-275.27566582
MoS_2	-87.17636874
MoS_2-H	-88.80608009
H	-0.02814307

References

[1] G. Kresse, J. Hafner, *Phys. Rev. B.*, 1993, **47**, 558–561.

[2] P.E. Blöchl, *Phys. Rev. B.*, 1994, **50**, 17953–17979.

[3] J.P. Perdew, K. Burke, M. Ernzerhof, *Phys. Rev. Lett.,* 1996, **77**, 3865–3868.

[4] J. Heyd, G.E. Scuseria, M. Ernzerhof, *J. Chem. Phys.,* 2003, **118**, 8207–8215.

[5] F. Zhang, H.Q. Zhuang, W. Zhang, J. Yin, F.H. Cao, Y.X. Pan, *Catal. Today.*, 2019, 203–208.

[6] D.A. Reddy, E.H. Kim, M. Gopannagari, R. Ma, P. Bhavani, D.P. Kumar, T.K. Kim, *ACS Sustain. Chem. Eng.,* 2018, **6**, 12835–12844.

[7] B. Archana, N. Kottam, S. Nayak, K.B. Chandrasekhar, M.B. Sreedhara, *J.Phys.Chem.C.*, 2020, **124**, 14485–14495.

[8] A. Kolivand, S. Sharifnia, , Int. J. Energy Res., 2021, **45**, 2739–2752.

[9] X. Huang, K. Wang, Y. Wang, B. Wang, L. Zhang, F. Gao, Y. Zhao, W. Feng, S. Zhang, P. Liu, *Appl. Catal. B Environ.,* 2018, **227**, 322–329.

[10] X. Wang, G. Liu, Z.G. Chen, F. Li, L. Wang, G.Q. Lu, H.M. Cheng*, Chem. Commun.,* 2009, 3452–3454

[11] B. Han, S. Liu, N. Zhang, Y.J. Xu, Z.R. Tang, *Appl. Catal. B Environ.*, 2017, **202**, 298–304.

[12] W.K. Jo, N.C. Sagaya Selvam, *Appl. Catal. A .*, 2016, **525**, 9–22.

[13] J. Chu, X. Han, Z. Yu, Y. Du, B. Song, P. Xu, *ACSAppl.Mater.Interfaces.*, 2018, **10**, 20404–20411.

[14] J. Zhang, Y. Wang, J. Jin, J. Zhang, Z. Lin, F. Huang, J. Yu, *ACSAppl.Mater.Interfaces.,* 2013, **5**, 10317–10324.

[15] Y. Zhang, W. Zhou, J. Wang, L. Jia, L. Liu, X. Tan, T. Yu, J. Ye, *J. Colloid Interface Sci.,* 2022, **607**, 769–781.

[16] X. Liu, C. Bie, B. He, B. Zhu, L. Zhang, B. Cheng, *Appl. Surf. Sci.*, 2021, **554**, 149622.

[17] K. He, L. Guo, *Int. J. Hydrog. Energy,* 2017, **42**, 23995–24005.

[18] F. Qiu, Z. Han, J.J. Peterson, M.Y. Odoi, K.L. Sowers, T.D. Krauss, *Nano Lett.*, 2016, **16**, 5347–5352.